Online Optimization in Closed Loop on the Power Flow Manifold

Adrian Hauswirth, Alessandro Zanardi, Saverio Bolognani, Florian Dörfler, and Gabriela Hug
Dept. of Information Technology and Electrical Engineering
ETH Zurich
Zurich, Switzerland
{hadrian,azanardi,bsaverio,dorfler,hug}@ethz.ch

***Abstract*—The focus of this paper is the online load flow optimization of power systems in closed loop. In contrast to the conventional approach where an AC OPF solution is computed before being applied to the system, our objective is to design an adaptive feedback controller that steers the system in real time to the optimal operating point without explicitly solving an AC OPF problem. Our approach can be used for example to simultaneously regulate voltages, mitigate line congestion, and optimize operating costs under time-varying conditions. In contrast to related work which is mostly focused on distribution grids, we introduce a modeling approach in terms of manifold optimization that is applicable in general scenarios. For this, we treat the power flow equations as implicit constraints that are naturally enforced and hence give rise to the power flow manifold (PFM). Based on our theoretical results for this type of optimization problems, we propose a discrete-time projected gradient descent scheme on the PFM. In this work, we confirm through a detailed simulation study that the algorithm performs well in a more realistic power system setup and reliably tracks the time-varying optimum of the underlying AC OPF problem.**

***Index Terms*—Load flow control, Manifold optimization, Gradient methods, Nonlinear dynamical systems.**

I. Introduction

In recent years, operating a power system has become more challenging as a consequence of ever increasing energy consumption, higher system complexity, decreasing timescales, energy-efficiency considerations, and most notably due to the integration of fluctuating and distributed renewable energy sources. This development has reinforced the interest in mathematical optimization for power system operations.

In particular, the increased volatility due to intermittent renewable infeed and changing consumption patterns have raised the ante on optimizing the system operation in real time based on live measurements [1]. This development is supported by the ubiquitous deployment of sensing equipment and controllable devices at all grid levels.

A straightforward approach to online optimization is to repeatedly apply conventional feedforward control (Fig. 1a). Based on a grid model and measurements of uncontrollable loads, dispatchable and non-dispatchable generators, an optimization problem is formulated and then solved using standard optimization algorithms. The result is then implemented by changing the set-points of controllable devices accordingly and the overall procedure is repeated again on regular time intervals. Although this approach is based on classical and well-understood methodologies from optimal power flow programming, it has some drawbacks that would hinder its successful application. In particular, this method is not robust with respect to model mismatch, since parameter uncertainties, time-varying loading and generation, and time delays between sensing and actuation would lead to steady-state errors (i.e., suboptimality) and violation of operational constraints.

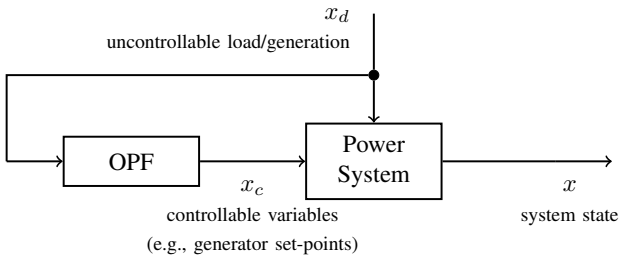

(a) Feedforward Power System Optimization

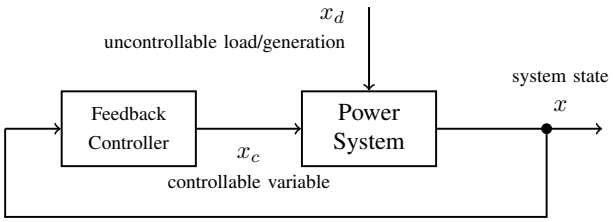

(b) Feedback Power System Optimization

Fig. 1. Online Power System Optimization Schemes

Instead, recent works such as [2]–[9] have proposed feedback controllers that steer the power system to an optimal state (Fig. 1b) without computing it explicitly by solving an OPF problem. We will refer to this concept as *feedback optimization*. In contrast to feedforward optimization, a feedback control loop is more robust towards parameter uncertainties, has no steady-state error and in general requires less computational effort. This latter feature is due to the idea that in feedback optimization the controller should be designed such that the physical system performs the most challenging

This research is supported by ETH Zürich funds and the SNF Assistant Professor Energy Grant #160573.

computational operations naturally. In the particular case of a power system, the AC power flow equations are one type of constraints that are naturally enforced by the laws of physics.

Previous works such as [2]–[4] base the control design on linearized models of the power flow equations around some fixed operating point, but then apply the controller in closed loop with the nonlinear physical system. In [5], the authors instead implicitly linearize the power flow equations at every iteration which enables more stringent optimality guarantees. All of these works are tailored to the specific requirements of distribution grids by considering for example only radial networks, PQ-buses and voltage constraints.

In this paper, we describe a general model for feedback optimization of power systems and provide a design method for discrete-time feedback controllers that are guaranteed to drive the system to an optimum of a given AC OPF problem. Our approach does not distinguish between meshed and radial networks, can incorporate various bus models as well as different types of operational constraints. This modeling flexibility and the general convergence guarantees are a consequence of our recent theoretical work [6].

By formalizing the feedback optimization task as a constrained optimization problem on the so-called *power flow manifold* (PFM), we treat the power flow equations already at the modeling stage as implicit constraints that cannot be violated. Any feedback law thus defines a vector field on the PFM. The properties of the algorithms in [2]–[4] are difficult to analyze if implemented in a feedback loop with the nonlinear system, since their design is not directly based on the PFM, and therefore the vector fields they induce on the PFM are somewhat contrived. We advocate that it is more natural to consider a canonical vector field on the PFM (e.g., the gradient descent minimizing a cost function on the PFM) and from this infer a discrete-time feedback controller.

The standard gradient descent on the PFM cannot directly handle operational constraints such as voltage or generation limits. We will therefore either model them as soft constraints or use the projected gradient descent depending on the nature of the constraint. We developed the theoretical underpinning of this approach in [6], where the continuous-time equivalent to this strategy has been proven to converge asymptotically to a feasible and locally optimal operating point.

In this paper, we show that the proposed controller also performs well under more realistic conditions, such as finite step-size, meshed grid topology, and different bus types. In particular, we confirm that the system is capable of tracking the optimal system state under fluctuating load and generation.

The rest of this paper is structured as follows: In Section II, we introduce the power system model. Besides defining the terms exogenous and endogenous variables, we formalize the operation that "naturally enforces" power flow constraints. In Section III, we present our feedback control law that steers the power system to an optimal state under stationary conditions, and in Section IV, we illustrate the behavior of the controlled power system in simulations.

II. Power Network Model

Consider a power grid with n buses and denote by $u_h \in \mathbb{C}$ and $s_h \in \mathbb{C}$ the voltage and power injection phasors at bus h. Voltages may be expressed in polar form as $u_h := v_h e^{j\theta_h}$ where v_h denotes the voltage magnitude and θ_h its angle, while for power injections we use rectangular coordinates $s_h := p_h + jq_h$ where p_h and q_h denote active and reactive power injections respectively. We use $u, s \in \mathbb{C}^n$ and $v, \theta, p, q \in \mathbb{R}^n$ to denote the vectors obtained from stacking the corresponding nodal quantities. We define

$$x := \begin{bmatrix} p \\ q \\ v \\ \theta \end{bmatrix} \in \mathbb{R}^{4n}$$

to represent the state of the power system. This augmented state allows us to accommodate multiple bus models and use an implicit description of the power flow equations.

Interconnections between buses are described by the standard Π-model for power transmission lines which gives rise to the bus admittance matrix Y. Nodal power injections and voltages are hence linked algebraically by the well-known AC power flow equations that take the form

$$\operatorname{diag}(u)\overline{Yu} - s = 0 \tag{1}$$

where $\operatorname{diag}(u)$ denotes the matrix with the elements of u on its diagonal.

A. The Power Flow Manifold

Consider the set of power system states that satisfy (1), i.e.,

$$\mathcal{M} := \{x \in \mathbb{R}^{4n} | F(x) = 0\} \ ,$$

where $F(x) : \mathbb{R}^{4n} \to \mathbb{R}^{2n}$ encodes the nonlinear equations (1), expressed in their real and imaginary parts. It has been shown in [10] that the set $\mathcal{M}$ has the structure of a smooth $2n$-manifold, or in other words, a $2n$-dimensional surface that is embedded in $\mathbb{R}^{4n}$. We call $\mathcal{M}$ the *power flow manifold*. The PFM describes the most fundamental physical constraints of power systems.

As a smooth manifold, $\mathcal{M}$ has a tangent space for every $x \in \mathcal{M}$ given by

$$T_x\mathcal{M} := \{w \in \mathbb{R}^{4n} | \nabla F(x) w = 0\}$$

where $\nabla F(x)$ denotes the Jacobian matrix of F at x. An explicit formula for $\nabla F(x)$ is given in [10], which contains (among others) the usual (DC) power flow linearizations at particular operating points.

B. Exogenous & Endogenous variables

For our feedback optimization we need to partition the state vector x into three subvectors each containing a specific type of variable. Namely, $x_c \in \mathbb{R}^r$ denotes the *controllable variables* and $x_d \in \mathbb{R}^s$ contains all variables that are governed by external processes but are not controllable. Together x_c and x_d form the *exogenous variables* x_{ex}. As a fact, we always have $r + s = 2n$. That is, the number of exogenous variables

matches exactly the dimension of the PFM. The remaining $2n$ variables are called *endogenous* and denoted by x_{end}.

The partition of the state variables into x_c, x_d and x_{end} is done by bus type as summarized in Table I. For a ***PQ generation*** bus i, active and reactive power generation p_i and q_i are controllable variables since they can be controlled directly via appropriate set-points, whereas v_i and θ_i will adapt autonomously to the current state of the grid. Hence they are endogenous. Similarly for a ***PV generation*** bus i the controllable variables are p_i and v_i while q_i and θ_i are endogenous. For a ***PQ load*** bus p and q are uncontrollable, but exogenous.

Finally, one node, here denoted by node 0, will act as the *slack bus* of the system. The voltage v_0 is controllable whereas θ_0 is uncontrollable since it will serve as the angle reference and will be set to 0. Although set-points for p_0 and q_0 can be defined, p_0 and q_0 are strictly speaking endogenous because by definition the slack bus power injections compensate for power imbalance rather than following its set-points. This is a crucial property for the retraction mechanism described Section III-A.

TABLE I
PARTITION OF STATE VARIABLES BY BUS TYPE

	Exogenous		Endogenous
	Controllable	Uncontrollable	
PQ generation	p_i, q_i		v_i, θ_i
PQ load		p_i, q_i	v_i, θ_i
PV generation	p_i, v_i		q_i, θ_i
slack bus	v_0	θ_0	p_0, q_0

C. Constrained optimal power flow

We assume that the power system is subject to operational constraints of the form

$$\begin{aligned} \underline{p}_i < p_i < \overline{p}_i \\ \underline{q}_i < q_i < \overline{q}_i \\ \underline{v}_i < v_i < \overline{v}_i \end{aligned}$$

for all nodes i and where $\underline{p}_i, \overline{p}_i, \underline{q}_i, \overline{q}_i, \underline{v}_i, \overline{v}_i$ denote upper and lower limits on active and reactive generation as well as voltage, respectively. Furthermore, we define the reference angle $\theta_0 = 0$ and line current limits of the form

$$|y_{kl}^{\text{sh}}|^2 v_k^2 + |y_{kl}|^2 (v_k^2 + v_l^2 - 4 v_k v_l \cos(\theta_{kl})) \leq \overline{I}_{kl}^2 \quad (2)$$

where y_{kl}^{sh} is the line shunt admittance, y_{kl} is the series admittance and $\overline{I}_{kl}$ is the current flow limit of the line from node k to l.

We classify the constraints according to the types of variables they contain. Constraints that depend only on exogenous variables form together the *feasible input region* $\mathcal{X} \subset \mathbb{R}^{2n}$. By the nature of exogenous variables, it is possible to strictly enforce these constraints at all times. In fact, our feedback control will output set-points that are guaranteed to lie in $\mathcal{X}$ by means of projections.

Contrarily, constraints on endogenous variables cannot be directly enforced. We propose to treat them as soft constraints. For this, assume that there are a total of m constraints on the endogenous variables, each given as $g_i(x_{\text{end}}) \leq 0$ for $i = 1, \ldots, m$. We define the penalty function

$$\phi(x_{\text{end}}) := \sum_{i=1}^{m} \gamma_i \max\{0, g_i(x_{\text{end}})\}^2 \quad (3)$$

where the $\gamma_i > 0$ are adjustable penalty parameters.

Consider a continuously differentiable cost function $J(x) : \mathbb{R}^{4n} \to \mathbb{R}$ depicting, e.g., the cost of generation. The sum of J and the penalty function (3) yields the objective function $\widetilde{J}(x) := J(x) + \phi(x_{\text{end}})$. Therefore, with our feedback controller we try to track the solution of

$$\begin{aligned} \underset{x \in \mathcal{M}}{\text{minimize}} \quad & J(x) + \phi(x_{\text{end}}) \\ \text{subject to} \quad & x_{\text{ex}} \in \mathcal{X} \end{aligned} \quad (4)$$

which is effectively an AC OPF problem where a subset of its constraints is treated as soft constraints.

III. Feedback Control Law

To minimize $\widetilde{J}$ subject to all exogenous constraints as in (4), we propose the update rule for the control variables given by

$$x_c^{k+1} = x_c^k + d_c^k \ . \quad (5)$$

The step d_c^k is given as the controllable subvector of the solution of

$$\underset{d^k \in \mathbb{R}^{4n}}{\text{minimize}} \quad ||d^k + \alpha \nabla \widetilde{J}(x^k)||^2 \quad (6a)$$

$$\text{subject to} \quad \nabla F(x^k) d^k = 0 \quad (6b)$$

$$x_{\text{ex}}^k + d_{\text{ex}}^k \in \mathcal{X} \ . \quad (6c)$$

where $\alpha > 0$ is a fixed step size parameter and $\nabla \widetilde{J}(x)$ denotes the gradient of the object function $\widetilde{J}(x)$ at $x \in \mathcal{M}$.

In a nutshell, the solution of the quadratic program (6) is the best feasible descent step in the direction of $\widetilde{J}$. This is illustrated in Fig. 2.

A feasible descent step has to lie in the tangent space of the PFM which is stated in constraint (6b). Furthermore, the descent step has to result in a state that satisfies the feasible input region. This is enforced by constraint (6c).

It can be shown that if $\alpha \to 0$ then (5) is equivalent to a continuous-time *projected gradient descent system*. In particular, we proved in [6] that these types of dynamical systems are well-behaved in the sense that trajectories converge to equilibrium points (i.e., no periodic orbits can occur) and an isolated equilibrium point is asymptotically stable if and only if it minimizes $\widetilde{J}$.

A. Natural retraction onto the PFM

Based on the proposed control architecture in Fig. 1b, we realize that we can actuate the system by updating the set-points x_c according to (5). However, even though the update step is tangential to $\mathcal{M}$ the new point $\tilde{x}$ as shown in Fig. 2 is in general not in $\mathcal{M}$.

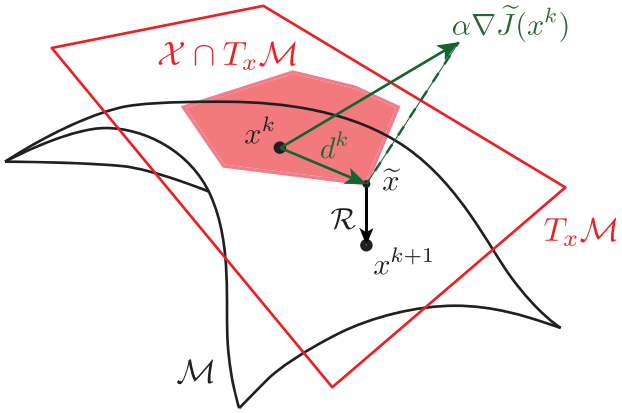

Fig. 2. Illustration of control and retraction mechanisms. The quadratic program (6) projects the scaled gradient $\alpha\nabla\widetilde{J}(x^k)$ to the feasible subset of the tangent plane $T_x\mathcal{M}$ resulting in the vector d^k. The point $x^k + d^k$ does in general not lie on $\mathcal{M}$, i.e., does not satisfy the power flow equations. Hence, the retraction $\mathcal{R}$ applied to that point produces x^{k+1} by adjusting all endogenous variables such that the power flow equations hold again.

In practice, the inherent power system dynamics will reestablish $x \in \mathcal{M}$, resulting in a change of the endogenous variables x_{end}. In other words, after changing generator setpoints the remaining variables will adapt automatically such that the power flow equations remain satisfied. These facts have been rigorously shown in the limit when the update steps are taken infinitesimally small [6].

We call this process of automatically enforcing the power flow equations a *retraction*. This notion is inspired by a similar notion in manifold optimization [11], [12], yet our use of the term is relatively informal.

We denote the retraction operation by $\mathcal{R} : \mathcal{M} \times \mathbb{R}^r \times \mathbb{R}^s \to \mathcal{M}$ that maps $(x, \tilde{x}_c, \tilde{x}_d)$ to a new state x' such that $x'_c = \tilde{x}_c$ and $x'_d = \tilde{x}_d$. For this to be well-defined, it is sufficient to assume that the power flow equations are solvable and the power flow Jacobian is non-singular everywhere on the feasible input region [6]. Concretely, for all possible values in the feasible input region, a power flow solution must exist and no voltage collapse can occur.

IV. Simulations

To test the proposed feedback controller, we have implemented a simulation procedure according to Fig. 3, with both the controller and the retraction implemented *in silico*. Concretely, the retraction $\mathcal{R}$ is performed using an off-the-shelf AC power flow solver, fixing the exogenous variables x_c to the new control inputs, enforcing the externally controlled variables x_d based on given time-varying profiles, and then computing the remaining values (i.e., the endogenous variables x_{end}). As discussed in Section III-A, this retraction step would not be part of the algorithm in real implementations, and instead would be "outsourced" to the physics of the power system.

In the following, we demonstrate the capabilities of our feedback controller, namely we show how our approach can be used to simultaneously regulate voltages throughout the network, mitigate line congestion and optimize operating costs.

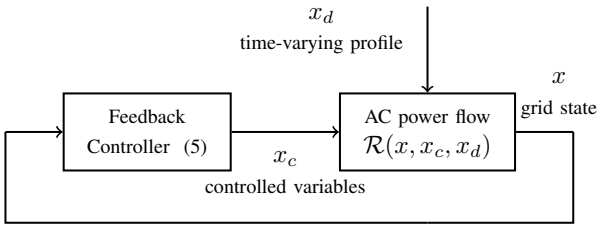

Fig. 3. Feedback OPF simulation process

For this, we consider a setup based on the IEEE 30 bus power flow test case [13] and time series data from [14]. For the power flow calculations that are part of the retraction operation the AC power flow solver of [15] is used.

The topology of the network is shown in Fig. 4. For simplicity, line shunts have been removed and transformers are at their nominal setting. The remaining grid parameters correspond to the original IEEE 30 bus test case.

All buses host some uncontrollable PQ loads. The total time-varying demand is given in Fig. 5, and represents ensembles of different types of loads (residential, industrial, commercial, agricultural).

In addition to the two conventional generators and three synchronous condensors in the original test case, a solar farm and wind power plant have been added at buses 8 and 25, respectively. These intermittent generators are subject to time-varying maximum active power injections $\overline{p}_s(t)$ and $\overline{p}_w(t)$ that model the fluctuating solar irradiation and prevalence of wind throughout the day. These profiles are also shown in Fig. 5.

All generators incur a cost in [$/hr] given as $a_i^{(1)} p_i + a_i^{(2)} p_i^2$. The marginal operating cost of the two renewable generators is set to 0.

Concerning reactive power generation, we make the simplifying assumption that the limits for the solar and wind farms are independent of their active power generation, i.e., there is no constraint on the power factor of the generator output. All generator parameters are summarized in Table II.

TABLE II
Generator cost coefficients, output constraints and bus type

	Cost		Constraints				
	$a^{(1)}$	$a^{(2)}$	$\underline{p}_i$	$\overline{p}_i$	$\underline{q}_i$	$\overline{q}_i$	Type
Generator 1	0.1	0.9	0	150	−40	50	slack
Generator 2	0.04	0.5	0	120	−40	50	PV
Condensor 1	0	0	0	0	−40	50	PV
Condensor 2	0	0	0	0	−40	50	PV
Condensor 3	0	0	0	0	−40	50	PV
Solar	0	0	0	$\overline{p}_s(t)$	−40	50	PQ
Wind	0	0	0	$\overline{p}_w(t)$	−40	50	PQ

Cost coefficients $a^{(1)}$ and $a^{(2)}$ are given in [$/(MW^{2}h)] and [$/MWh] respectively. Power generation limits are in [MW] and [MVar] accordingly.

Further constraints include upper and lower voltage limits of 1.06 p.u. and 0.94 p.u. at every bus, branch current limit of 0.9 p.u. for the line from bus 8 to bus 9 and a similar limit of 0.8 p.u. for the line from bus 24 to bus 25.

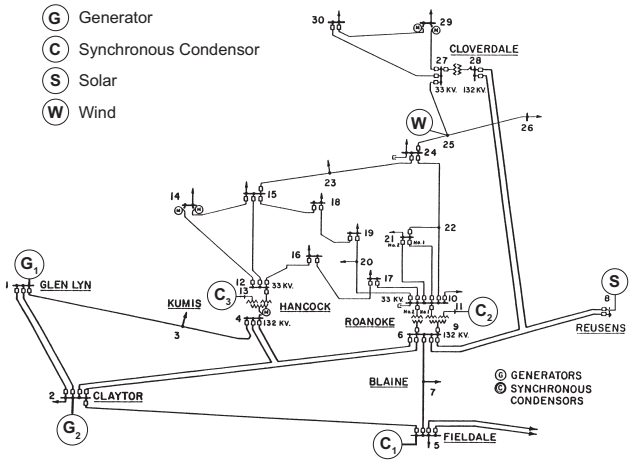

Fig. 4. IEEE 30 bus system with additional intermittent generation

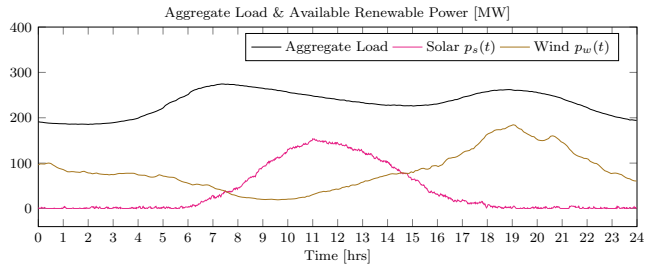

Fig. 5. Available solar and wind power and aggregate fixed load over 24 hours

We simulate 24 hours of operation. Every 15 seconds, the controller receives field measurements about the system state x^k, solves the quadratic program (6), and updates the set-point of the controllable generators via (5) for the next iteration. At that stage the retraction $\mathcal{R}$ is performed, that is, the AC power flow solver computes feasible system state based on the new generator set-points. After this, the controller receives the new measurements. Note that this procedure implies a 15 second delay between sensing and actuation.

The result of the simulation is shown in Fig. 6. In order to evaluate how well the optimum of a the underlying AC OPF problem is tracked under time-varying conditions, we also compute the generation cost that corresponds to the optimal operation of the grid, as if we had infinite computational power and perfect model knowledge, and we could sense, compute and actuate it in real time (i.e., without time delay). The comparison in Fig. 6a between the generation cost achieved by the feedback optimization approach and the offline OPF computation demonstrates the excellent tracking performance in terms of generation cost.

Bus voltage profiles and the global voltage constraints are shown in Fig. 6b. The voltage profiles at generator buses are highlighted in color.

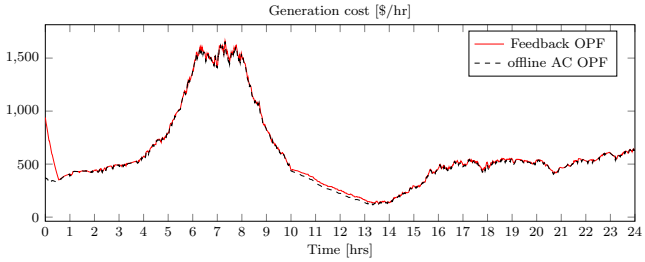

(a) Generation cost achieved in closed loop and with offline AC OPF

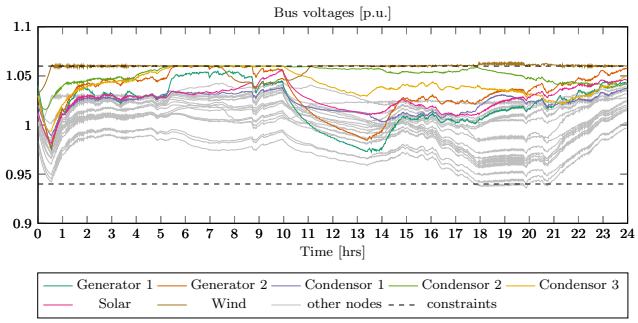

(b) Voltage profiles in closed loop

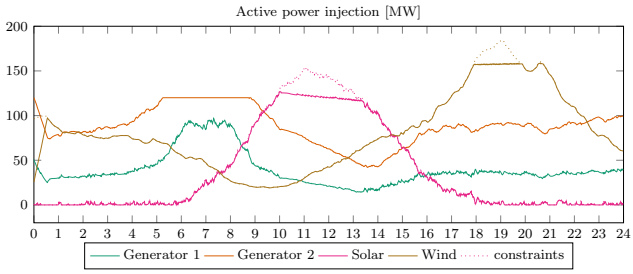

(c) Active power generation profiles in closed loop

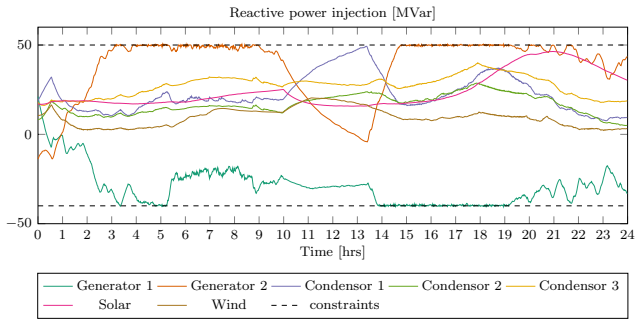

(d) Reactive power generation profiles in closed loop

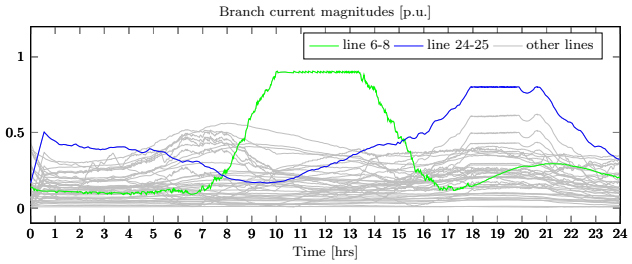

(e) Example of line congestion handling in closed loop

Fig. 6. Simulation results for 30 bus test case over 24 hours

Fig. 6c and 6d show active and reactive power generation respectively. For the active power generation of renewable energy sources, the available power is drawn as a dotted line to highlight curtailment.

Finally, Fig. 6e shows line currents. Since all transformers and line shunts have been removed all lines conserve current, i.e., there is no need to distinguish between "to" and "from" currents. The two lines whose limits become active over the simulation horizon are highlighted.

The simulation unfolds as follows. From 00:00 to about 00:30 converges to the optimal operating point before starting to track it. This transitory phenomenon is a consequence of a highly suboptimal initialization point and can be completely avoided by using an AC OPF solution computed offline as an initial point for the simulation. It does not occur in continuous operation. We show this behavior to demonstrate that our algorithm creates a large region of attraction and converges reliably to the optimum even from far away operating points.

At about 07:00 in the simulation the consumption reaches a first maximum while wind and solar generation are low. Consequently, Generator 2 runs at full capacity and the most expensive generator, Generator 1, has to ramp up to cover the remaining load resulting in high generation costs for this time period.

With the appearance of abundant solar power generation generation cost decreases sharply. From about 10:00 to 13:00 the line from the solar power plant to the adjacent bus 8 works is congested and as a consequence solar power output is curtailed.

During the period from 18:00 to 20:00 the high availability of wind power leads to over-voltage and line congestion problems leading to multiple active constraints. The controller adapts the generators set-point by first using the available reactive power resources to regulate the voltage, and finally by curtailing the wind production.

The small residual violation of endogenous constraints (in particular of the voltage band) is an inherent result of using soft penalty functions for voltage constraints. This violation can be reduced by increasing the penalty terms, at the cost of a more aggressive actuation.

In this context it must be noted that strict constraint satisfaction of voltage and line constraints in a feedback optimization context is neither sensible nor practical. In any real-world application subject to model uncertainty, time delays and measurement errors slight constraint violations are bound to happen with any online optimization approach.

Overall, the feedback controller prioritizes cheap generators whenever possible and available to minimize generation cost. It acts on reactive power generation and curtails active power dynamically within its limits to ensure that voltage and line constraints across the grid are respected.

V. Conclusions

In this work, we have presented a novel framework for the design of feedback controllers for power system online operation. The proposed framework allows to derive mathematically rigorous guarantees of convergence to the solution of an optimal nonlinear AC power flow program. The resulting feedback strategy is therefore capable of tracking the time-varying optimal operating point of the grid, while enforcing operational constraints along the entire trajectory of the system.

The proposed feedback controller can fully exploit the nonlinear nature of the system (therefore integrating multiple ancillary services such as voltage regulation, economic dispatch, congestion control, etc.) although it does not rely on computational tools such power flow or OPF solvers.

In future work, we will address the robustness and adaptivity properties of the proposed scheme with respect to model uncertainties and approximate updates. Another avenue of future research is to extend our algorithmic procedure to dualization methods and compare their performance with the soft penalties investigated here.

References

[1] J. A. Taylor, S. V. Dhople, and D. S. Callaway, "Power Systems Without Fuel," *arXiv:1506.04799 [cs.SY]*, Jun. 2015.

[2] S. Bolognani and S. Zampieri, "A distributed control strategy for reactive power compensation in smart microgrids," *IEEE Trans. on Automatic Control*, vol. 58, no. 11, Nov. 2013.

[3] S. Bolognani, G. Cavraro, R. Carli, and S. Zampieri, "Distributed reactive power feedback control for voltage regulation and loss minimization," *IEEE Trans. on Automatic Control*, vol. 60, no. 4, Apr. 2015.

[4] E. Dall'Anese and A. Simonetto, "Optimal Power Flow Pursuit," *arXiv:1601.07263 [math]*, Jun. 2016.

[5] L. Gan and S. H. Low, "An Online Gradient Algorithm for Optimal Power Flow on Radial Networks," *IEEE J. on Selected Areas in Communications*, vol. 34, no. 3, Mar. 2016.

[6] A. Hauswirth, S. Bolognani, G. Hug, and F. Dörfler, "Projected gradient descent on Riemannian manifolds with applications to online power system optimization," in *2016 54th Annual Allerton Conference on Communication, Control, and Computing (Allerton)*, Sep. 2016.

[7] N. Li, L. Chen, C. Zhao, and S. H. Low, "Connecting automatic generation control and economic dispatch from an optimization view," in *American Control Conference (ACC), 2014*. IEEE, 2014.

[8] E. Dall'Anese, S. V. Dhople, and G. B. Giannakis, "Photovoltaic inverter controllers seeking ac optimal power flow solutions," *IEEE Transactions on Power Systems*, vol. 31, no. 4, July 2016.

[9] D. B. Arnold, M. Negrete-Pincetic, M. D. Sankur, D. M. Auslander, and D. S. Callaway, "Model-free optimal control of var resources in distribution systems: An extremum seeking approach," *IEEE Transactions on Power Systems*, vol. 31, no. 5, Sept 2016.

[10] S. Bolognani and F. Dörfler, "Fast power system analysis via implicit linearization of the power flow manifold," in *53rd Annual Allerton Conference on Communication, Control, and Computing*, Sep. 2015.

[11] P.-A. Absil, R. Mahony, and R. Sepulchre, *Optimization algorithms on matrix manifolds*. Princeton, N.J. ; Woodstock: Princeton University Press, 2008.

[12] P.-A. Absil and J. Malick, "Projection-like Retractions on Matrix Manifolds," *SIAM Journal on Optimization*, vol. 22, no. 1, Jan. 2012.

[13] "Power Systems Test Case Archive, University of Washington, Electrical Engineering," 2007. [Online]. Available: http://www.ee.washington.edu/research/pstca/

[14] "Wind generation & total Load in the BPA balancing authority," 2016. [Online]. Available: https://transmission.bpa.gov/business/operations/wind/

[15] R. D. Zimmerman, C. E. Murillo-Sanchez, and R. J. Thomas, "MATPOWER: Steady-State Operations, Planning, and Analysis Tools for Power Systems Research and Education," *IEEE Transactions on Power Systems*, vol. 26, no. 1, Feb. 2011.